Shallow Ti
LiNbO 3 strip waveguide

Hua, Ping-Rang; Chen, Bei; Zhao, Quan-Zhou; Han, Fang; Yu, Dao-Yin; Pun, Edwin Yue-Bun; Zhang, De-Long

Published in:
IEEE Photonics Journal

Published: 01/01/2012

Document Version:
Final Published version, also known as Publisher's PDF, Publisher's Final version or Version of Record

Published version (DOI):
10.1109/JPHOT.2012.2192722

Publication details:
Hua, P-R., Chen, B., Zhao, Q-Z., Han, F., Yu, D-Y., Pun, E. Y-B., & Zhang, D-L. (2012). Shallow Ti: LiNbO 3 strip waveguide. *IEEE Photonics Journal*, *4*(2), 520-527. [6178755].
https://doi.org/10.1109/JPHOT.2012.2192722

IEEE Photonics Journal
An IEEE Photonics Society Publication

Shallow Ti:$LiNbO_3$ Strip Waveguide

Volume 4, Number 2, April 2012

Ping-Rang Hua
Bei Chen
Quan-Zhou Zhao
Fang Han
Dao-Yin Yu
Edwin Yue-Bun Pun, Senior Member, IEEE
De-Long Zhang

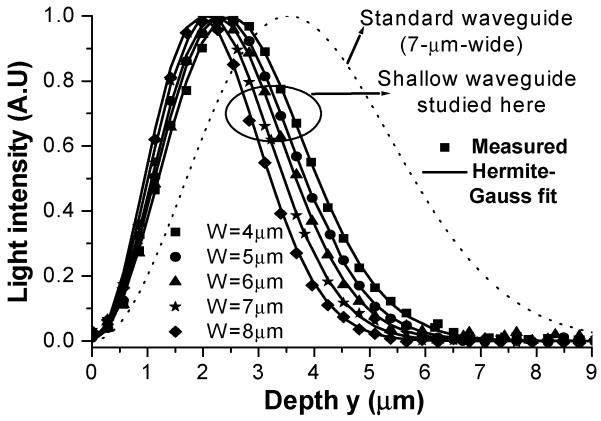

DOI: 10.1109/JPHOT.2012.2192722
1943-0655/$31.00 ©2012 IEEE

Shallow Ti:$LiNbO_3$ Strip Waveguide

Ping-Rang Hua,[1,2,3] Bei Chen,[1,2,3] Quan-Zhou Zhao,[1,2,4] Fang Han,[1,2] Dao-Yin Yu,[1,2] Edwin Yue-Bun Pun,[3] *Senior Member, IEEE*, and De-Long Zhang[1,2,3]

[1]School of Precision Instruments and Opto-electronics Engineering, Tianjin University, Tianjin 300072, China
[2]Key Laboratory of Optoelectronic Information Technology, Ministry of Education, Tianjin University, Tianjin 300072, China
[3]Department of Electronic Engineering, City University of Hong Kong, Kowloon, Hong Kong
[4]School of Physics and Electronic Engineering, University of Shanxi Datong, Datong 037009, China

DOI: 10.1109/JPHOT.2012.2192722

Manuscript received March 5, 2012; accepted March 26, 2012. Date of current version April 6, 2012. This work was supported by the National Natural Science Foundation of China under Project 50872089, Project 61077039, and Project 61107056; by the Key Program for Research on Fundamental to Application and Leading Technology, Tianjin Science and Technology Commission of China under Project 11JCZDJC15500; and by Specialized Research Fund for the Doctoral Program of Higher Education of China under Project 20100032110052. Corresponding author: D.-L. Zhang (e-mail: dlzhang@tju.edu.cn).

Abstract: We report shallow single-mode Ti:$LiNbO_3$ strip waveguides fabricated on Z-cut congruent $LiNbO_3$ substrate by a two-step Ti-diffusion process, starting with the diffusion of a homogeneous Ti film at 1020 °C for 2 h, followed by the diffusion of Ti strips at the same temperature for 2 h again. These waveguides with a loss as low as 0.3 dB/cm have smaller cross section sizes, larger surface refractive index increment, and a mode field depth that is half as shallow as the conventional Ti:$LiNbO_3$ waveguide, satisfying the requirement by photonic crystal fabrication. The Ti^{4+}-concentration profile was characterized by secondary ion mass spectrometry. The 2-D refractive index profile model is proposed for the peculiar waveguide structure. On the basis of the index model, we have simulated the mode field distribution using the beam propagation method. The results show that the theory is in good agreement with the experiment, verifying the validity of the proposed index model.

Index Terms: Ti:$LiNbO_3$ strip waveguide, photonic crystal.

1. Introduction

The photonic crystal (PhC) displays a number of advantages, such as large surface-volume ratio, substantial size reduction, and peculiar manipulation for transmitted photons. It has given birth to a number of realizations such as lowering energy loss, increasing operation speed, and realizing new functions of related devices. Moreover, integration of PhCs within a planar waveguide enables to implement compact devices with fully integrable functions. In these devices, the light is confined into the crystal by a classical waveguide structure. Their tunability is realized by means of an active substrate in which the optical properties can be modified by external parameters like the electric field, temperature, strain, etc. Among different types of active materials, $LiNbO_3$ (LN) is an attractive substrate material for 2-D PhCs because of its high refractive index and excellent electrooptic (EO), acoustooptic, and nonlinear optical properties. Over the past few years, great effort has been made to explore a feasible way to implement a PhC structure within the LN waveguide. Researchers have demonstrated their implementation of the PhC in a proton exchanged (PE) LN waveguide using focused ion beam milling [1], [2], reactive ion etching [3], and inductively coupled plasma [4] methods.

Nevertheless, the fabrication of satisfied PhC structure in LN continues to be a difficult task. One major problem is that the designed diameter of the etched holes retains only to an etching depth of ~ 2 μm. Deeper than 2 μm, the holes drilled are no longer cylindrical but become a conical shape due to the charge accumulation effect arising from the insulating property of LN. This experimental limitation requires a shallower waveguide. As a shallow waveguide on LN can be easily fabricated by the PE method, previous studies were all based upon the PE LN waveguide. It is well known that the PE LN waveguide suffers from the degradation of EO coefficient, instability, larger waveguide loss, and complicated crystalline phase in the waveguide layer. In contrast, the Ti-diffused LN (Ti:LN) waveguide has of a number of advantages over the PE waveguide such as lower waveguide loss, higher thermal, electric and chemical stabilities, retained crystalline phase, and, hence, EO property. All of the problems concerning with PE waveguide can be avoided if a Ti:LN waveguide is used to develop a PhC device. However, the conventional Ti:LN strip waveguide, which is usually fabricated by indiffusion of a 6–8-μm-wide, 90–110-nm-thick Ti strip at 1030–1060 °C for 9–10 h in the argon atmosphere, is not suitable for development of PhC device as it has a 1/e transverse magnetic (TM) mode field depth of 5 μm [5] [Transverse electric (TE) mode has a larger mode size.] A shallow Ti:LN strip waveguide is required and desired. In this letter, we report shallow Ti:LN strip waveguides on Z-cut congruent LN substrate. The waveguides were fabricated by a special two-step method: diffusion of the homogeneously coated Ti film at first and then the photolithographically patterned Ti strips.

2. Experiment

The waveguide fabrication started from a Z-cut congruent LN with a two-step technological process of Ti diffusion. First, a 40-nm-thick Ti metal film was coated onto one surface of the 0.5-mm-thick congruent substrate followed by a diffusion at 1020 °C for 2 h in surrounding air. Second, a number of Ti strips, with an initial thickness of 56 nm and initial widths of 4, 5, 6, 7, and 8 μm, were photolithographically delineated on the surface followed by a diffusion again at 1060 °C for 2 h in air. Accordingly, a special waveguide structure of the strip waveguides embedded in a planar waveguide is formed. Note that we are more interested in the strip waveguides.

A time-of-flight second ion mass spectrometry (ION-TOF TOF SIMS V) was used to analyze the surface profile of Ti ions and the depth profiles of all of the substrate ions ^{7}Li, ^{93}Nb, ^{16}O and the doping ion ^{48}Ti inside or outside the 6-μm-wide strip waveguide. The surface profile was obtained by doing surface mapping with a raster size of 151.4×151.4 μm^2. For the depth analysis, a Cs^+-beam (~ 45 μm in diameter) of 32 nA at 3 keV was used to sputter a crater of 150×150 μm^2, and a pulsed bismuth ion beam (pulsed current: 1 pA, pulsed energy: 25 keV) was used to analyze the secondary ions of ^{7}Li, ^{93}Nb, ^{16}O, and ^{48}Ti as a function of time. Positive secondary ions were detected. Ions from a central area of 3×3 μm^2 inside the erosion crater rastered on the strip waveguide and 27.3×27.3 μm^2 inside the erosion crater rastered on the planar waveguide area were detected. A low energy pulsed electron gun was used to reduce the surface charge accumulation during the analysis. For the same purpose, before the SIMS analysis a 30-nm-thick Ag film was coated onto the surface of each sample to be analyzed. The trace and the depth of each erosion crater were measured by a Tencor Alpha Step 200 profilometer. The depth resolution was mainly determined by the roughness of the crater under analysis and is better than 5 nm in our case.

3. Results and Discussion

After the diffusion processes, the strip waveguides were checked by an optical microscope. As the representative, Fig. 1 shows the morphology image of the 6-μm-wide shallow Ti:LN strip waveguide. The crystallographic axes are indicated. After the fine polish to the two endfaces of the sample, the strip waveguides were optically characterized. End-fire coupling was carried out by launching into the 1.2-cm-long strip waveguides a 1.5-μm light. Guiding exists in all strip waveguides. Both TM and TE modes are well guided. As expected, the waveguides confine the TM mode strongly while the TE mode weakly. In the following, we focus our attention on the TM modes.

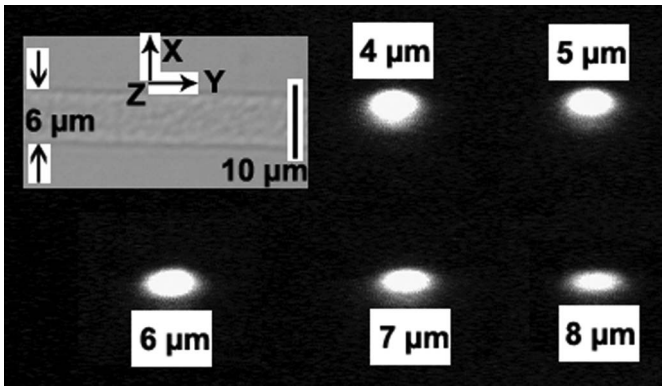

Fig. 1. Morphology image of 6-μm-wide shallow Ti:LN strip waveguide (left upper corner) and near-field patterns of TM mode guided in the 4, 5, 6, 7, and 8-μm-wide waveguides at 1.5-μm wavelength.

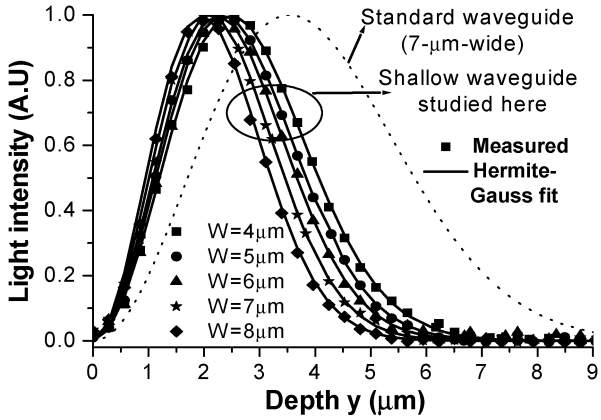

Fig. 2. Measured (scattered symbols) and Hermite–Gauss-fitting (solid lines) field depth profiles of TM modes guided in the strip waveguides with different initial Ti-strip widths. For comparison, the field profile of the TM mode guided in a conventional waveguide is also shown (dotted plot).

Fig. 1 shows the near-field patterns of TM modes guided in the 4, 5, 6, 7, and 8-μm-wide waveguides at the 1.5-μm wavelength. All guides are single mode at 1.5 μm. Further mode pattern analysis shows that, like in the case of conventional Ti:LN strip waveguide, the light intensity of mode guided in the waveguides under study follows a Gauss function $A_x \exp(-2(x/W_x)^2)$ in the width direction x and a Hermite–Gauss function $A_y y^2 \exp(-2(y/W_y)^2)$ in the depth direction y. (For convenience, here, we consider an $x-y$ Cartesian reference frame fixed at the center of the strip guide surface with the x axis along the width direction and the y axis pointing to the depth direction of the guide.) At the 1.5 μm wavelength, the TM mode size W_x (W_y) is 3.3 (3.5), 3.6 (3.3), 3.9 (3.2), 4.2 (3.0), and 4.4 (2.8) $\pm$ 0.1 μm for the 4-, 5-, 6-, 7-, and 8-μm-wide guides, respectively. In contrast, the TE mode size is considerably larger than the TM mode size due to the weaker guiding strength for this polarization. For the TE mode guided in the 7-μm-wide guide, its size is $7.0(4.5) \pm 0.1$ μm. We are more interested in the mode field profile in depth direction. Fig. 2 shows the measured (scattered symbols) and Hermite–Gauss-fitting (solid lines) field depth profiles of TM mode (at 1.5-μm wavelength) guided in the waveguides with different initial Ti-strip widths. For comparison, we also dot-plot the field profile of TM mode guided in a conventional strip waveguide fabricated by diffusion of 7-μm-wide, 95-nm-thick Ti strip at 1030 °C for 9 h in argon atmosphere [5]. As expected [6], the depth mode size decreases with the increased Ti-strip width. For the 6-, 7-, or 8-μm-wide guide, the depth TM mode size, which is around 3 μm, is considerably smaller than that

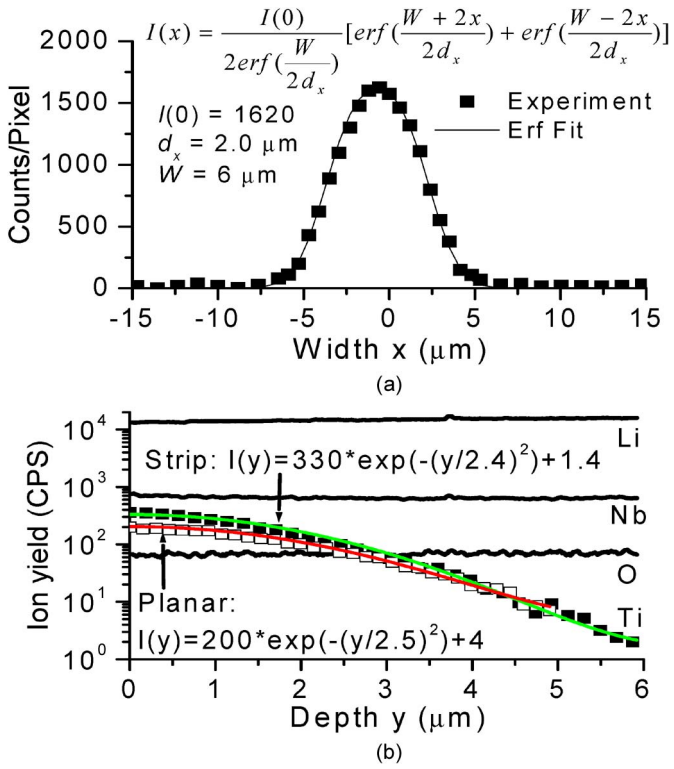

Fig. 3. (a) Surface ^{48}Ti profile (full squares) of the 6-μm-wide Ti:LN strip waveguide. (b) Depth profiles of ^{6}Li, ^{93}Nb, ^{16}O, and ^{48}Ti (full squares) in same strip waveguide. The open squares denote the Ti^{4+} profile in the planar waveguide area. The colored curves represent the Gaussian fitting results.

of the conventional waveguide: $\sim$5 μm [5]. It is thus concluded that our 6-, 7-, or 8-μm-wide guides are about 40% shallower than the conventional guide. From the viewpoint of PhC fabrication, the holes can be drilled down to a depth of $\sim$4 μm [7]. One can see from Fig. 2 that the TM mode guided in the 6-, 7-, or 8-μm-wide waveguide is almost entirely confined within the 4-μm depth range, matching well with the requirement of PhC fabrication and confirming the validity of the waveguides.

Next, we pay attention to the profile characteristics of diffused Ti^{4+} ions and refractive index in the planar and strip waveguide layers. The Ti^{4+}-concentration profile was analyzed by secondary ion mass spectrometry (SIMS). Fig. 3(a) shows the Ti^{4+}-concentration profile (full squares) mapped from the 6-μm-wide strip waveguide surface. Regarding the surface Ti^{4+}-concentration profile, there is one point to be clarified. In principle, there must be a contribution of the planar waveguide to the profile. However, one can see from Fig. 3(a) that the profile levels off at zero. This is related to the surface mapping experiment, which depends just only on the gray scale of the waveguide surface. As the strip waveguide has an obvious graded change of gray scale, its surface mapping is thus successful. Instead, the mapping for the planar waveguide surface is impossible as one cannot observe an obvious gray scale change. Therefore, the surface Ti^{4+}-concentration profile in Fig. 3(a) does not include the contribution from the planar waveguide. Like the conventional waveguide [8], the Ti^{4+}-concentration profile on our shallow strip guide surface also follows a sum of two error functions. The solid-line represents the fitting result. The fitting expression and parameters are indicated in Fig. 3(a). In the fitting expression, the W represents the initial Ti-strip width, and the d_x denotes the diffusion width having a value of 2.0 ± 0.2 μm. Fig. 3(b) shows the measured depth profiles of substrate ions ^{7}Li, ^{93}Nb, ^{16}O and diffused ^{48}Ti ions (full squares) in the same 6-μm-wide strip waveguide. The open squares denote the Ti^{4+} profile measured from the planar waveguide area. Like the conventional waveguide [8], the Ti^{4+} ions in the diffusion depth direction also follow

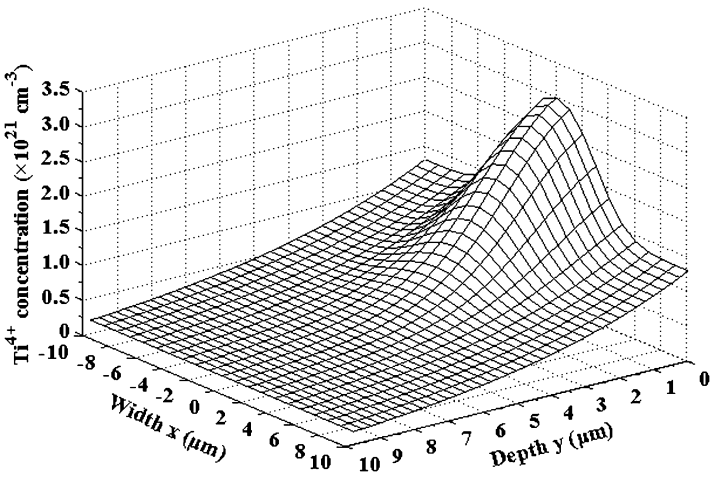

Fig. 4. Surface plot of 2-D Ti^{4+}-concentration in the 6-μm-wide shallow strip waveguide.

the traditional Gaussian profile whether the ions are in the strip or in the planar waveguide area. The colored curves represent the Gaussian fitting results. The fitting expressions and parameters are indicated. The 1/e Ti^{4+} diffusion depth, named d_y, is 2.4 ± 0.2 μm in the strip guide layer and 2.5 ± 0.2 μm in the planar guide layer, which can be regarded as identical within the error. The diffusion width (depth) value yields a width (depth) diffusivity of $0.5 \pm 0.1 (0.4 \pm 0.1)$ μm^2/h, which is in good agreement with the result 0.5 (0.4) and 0.3 (0.4) μm^2/h, evaluated using the diffusion constant and activation energy reported by Fukuma and Noda [8] and by Fouchet *et al.* [9], respectively.

The d_x and d_y values show that the waveguides studied here are narrower and shallower than the conventional waveguide, which has a $1/e$ diffusion width (depth) of 4–5 (6–7) μm. The reason why such a narrow and shallow strip guide can support single mode at 1.5 μm is that the guide has a higher surface Ti^{4+}-concentration and, hence, a larger surface index increment. Next, we try to establish the refractive index profile model of the special shallow strip waveguide structure. The 2-D Ti^{4+}-concentration profile in the strip waveguide layer can be expressed as

$$C_{\mathrm{Ti}}(x,y) = 0.5C_1[\mathrm{erf}((W+2x)/(2d_x)) + \mathrm{erf}((W-2x)/(2d_x))]\exp\left(-(y/d'_y)^2\right)/\mathrm{erf}(W/(2d_x)) + C_2\exp\left(-(y/d_y)\right)^2 \quad \text{for } -\infty < x < +\infty \quad \text{and} \quad y > 0 \quad (1)$$

where the first term is the contribution due to the 2-h diffusion of 56-nm-thick Ti strip, and the second term is the contribution due to the 4-h diffusion of 40-nm-thick homogeneous Ti film. Note that the aforementioned diffusion depth d_y in the strip guide is actually that in the planar waveguide, which corresponds to a longer diffusion time of 4 h. While the d'_y in (1) corresponds to a shorter diffusion time of 2 h and is different from the d_y, it can be evaluated from the known diffusivity (0.4 μm^2/h) and has a value of ~ 1.8 μm. As an example, in Fig. 4 we show the surface plot of 2-D Ti^{4+}-concentration in the 6-μm-wide strip waveguide. The Ti^{4+}-concentration is about 1.0×10^{21} ions/cm^3 on the planar waveguide surface and 3.0×10^{21} ions/cm^3 on the strip waveguide surface. Indeed, The Ti^{4+}-concentration on the strip waveguide surface is nearly three times higher than that of the conventional waveguide, $\sim 1.2 \times 10^{21}$ ions/cm^3 [10].

On the basis of (1), the Ti^{4+}-induced index increment $\Delta n\ (x, y)$ in the strip waveguide can be constructed as

$$\Delta n(x,y) = 0.5\Delta n_1[\mathrm{erf}((W+2x)/(2d_x)) + \mathrm{erf}((W-2x)/(2d_x))]\exp\left(-(y/d'_y)^2\right)/\mathrm{erf}(W/(2d_x)) + \Delta n_2\exp\left(-(y/d_y)\right)^2 \quad \text{for} \quad -\infty < x < +\infty \quad \text{and} \quad y > 0 \quad (2)$$

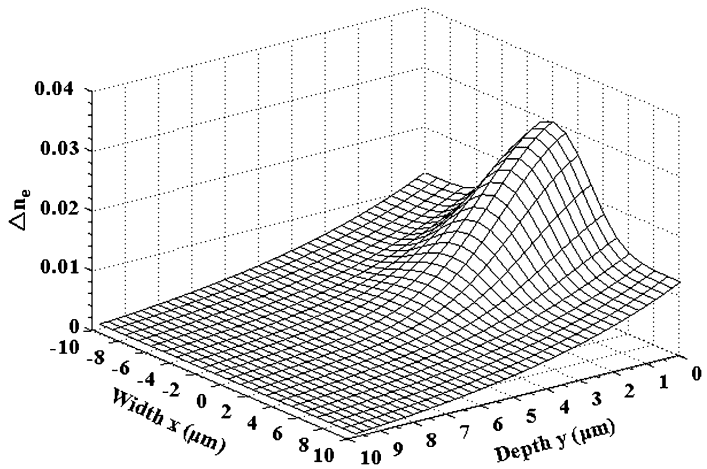

Fig. 5. Surface plot of 2-D Ti^{4+}-induced extraordinary index increment in the 6-μm-wide shallow strip waveguide.

where Δn_1 and Δn_2 are the Ti-induced surface index increments corresponding to 56- and 40-nm-thick Ti films, respectively. Note that the conventional waveguide is formed by diffusion of $\sim$100-nm-thick Ti strip and here the total Ti metal thickness coated onto the strip waveguide area is 96 nm. Both are nearly identical. The y-direction field is strongly confined due to the larger surface index increment arising from the shallow guiding layer. To avoid multimode propagation in the width direction, a planar waveguide was introduced to reduce the x-direction field confinement to the mode in strip waveguide. In fact, experimental results show that without introducing the planar waveguide, the strip waveguides fabricated under the same condition support two modes in the x direction. As a representative, in Fig. 5 we show the surface plot of 2-D Ti^{4+}-induced extraordinary index increment Δn_e in the 6-μm-wide strip waveguide. The Δn_e value is $\sim$0.01 on the planar waveguide surface and $\sim$0.03 on the strip waveguide surface. The latter is nearly three times larger than that of the conventional waveguide: $\sim$0.01 [9]. It should be pointed out that for the case of Δn_e, (2) can only be a rough approximation because the Δn_e is nonlinearly dependent on the Ti^{4+}-concentration [9].

On the basis of the refractive index model described by (2), we further simulated the fundamental TM mode field profiles using the 3-D beam propagation method (BeamPROP from RSoft Design Group, Inc.). The numerical results show that the simulated W_y value of the TM mode is about 3.5, 3.3, 3.1, 3.0, and 2.8 μm for the 4-, 5-, 6-, 7-, and 8-μm-wide guides, respectively, which are in good agreement with the corresponding experimental values 3.5, 3.3, 3.2, 3.0, and 2.8 $\pm$ 0.1 μm, respectively. The good agreement between the theoretical and experimental results gives a hint that the refractive index model proposed for the special shallow strip waveguide studied here is close to the practical scenario and, hence, is valid.

The loss figure is a key specification for an optical waveguide. It is well known that an accurate loss number should be determined by the Fabry–Perot method [11]. Due to the limited facilities, here, we only roughly evaluate the waveguide loss of the TM mode from the measured insertion loss. At 1.5-μm wavelength, the fiber-to-fiber insertion losses of the 4-, 5-, 6-, 7-, and 8-μm-wide, 1.2-cm-long guides were measured to be 6.8, 6.9, 6.8, 7.2, and 7.6 dB, respectively, which are higher than that of the aforementioned conventional waveguide: $\sim$5.0 dB. From the obtained mode sizes, the coupling loss between the waveguide and a single-mode fiber (with a mode field diameter of 10.3 μm) is 3.0, 3.1, 3.1, 3.2, and 3.4 dB, respectively, which are also higher than that of the aforementioned conventional guide: $\sim$2.0 dB. With ignored etalon effect, the total reflection loss of the two waveguide endfaces against the two fiber endfaces is 0.3 dB. The waveguide losses are then determined to be $\sim$0.40, 0.38, 0.29, 0.36, and 0.32 dB/cm, respectively, which are higher than the typical value of conventional guide: $\sim$0.2 dB/cm [10]. With optimized fabrication parameters, the loss could be reduced to a lower level.

In addition, it is also essential to pay attention to the situation of Li out-diffusion because no any Li out-diffusion suppression measure has been taken during the Ti diffusion procedure, which was carried out under the surrounding air. Here, the optical method of birefringence measurement was used to quantitatively evaluate the Li_2O-content at the surface of the sample studied. The n_o and n_e values at the undoped surface of the sample, where the material is clear LN, were measured using a Metricon 2010 prism coupler with an error of 1×10^{-3}. The birefringence value, given from an averaged result of the data measured at several different places of surface, is 0.0842, 0.0750, and 0.0732 at the wavelengths of 633, 1311, and 1550 nm, respectively. From the reported Li_2O content dependence of the birefringence of LN [12], the Li_2O content at the undoped surface is evaluated as 48.5 ± 0.1 mol%, which equals the nominal value of the as-grown material, indicating that the Li out-diffusion was not serious at the undoped surface though the anneal was carried out under the surrounding air. Obviously, we are more interested in the situation at the waveguide surface. Due to Ti-doping effect on the refractive index, we are unable to characterize the Li_2O content at the waveguide surface in a similar way. Nevertheless, one can anticipate that the situation at the waveguide surface should not have a large difference from that at the undoped surface because the diffusion temperature is not high, and the duration is not long: only 4 h in total.

Finally, we give an outline of the potential applications for the peculiar waveguide studied in this work. Besides the PhC application mentioned above, such waveguide may also find its use in other fields such as the generation of Terahertz and far-infrared waves on the basis of the quasi-phase matching concept of periodically poled LN waveguide [13]–[15], development of phase modulator or electrooptically modulated long period waveguide grating device [16]. Of course, like the conventional Ti-diffused strip waveguides, these shallow waveguides can be also used to develop various active Ti:Er:LN devices including lasers, amplifiers and various nonlinear integrated optical devices [17]–[21]. The nearly half shallower mode field distribution gives a hint that the profile of diffusion-doped rare-earth ions can be nearly half shallower than the case of utilizing the conventional waveguide, and hence, the diffusion duration of the rare-earth ions, which is usually longer than 100 h in the case of utilizing the conventional waveguide [17]–[21], could be shortened in a large scale.

4. Conclusion

We have demonstrated narrow and shallow Ti:$LiNbO_3$ strip waveguides fabricated by two-step Ti-diffusion processes with only 4 h diffusion time in total. The waveguides, well supporting single TM mode at 1.5 μm and having a loss as low as 0.3 dB/cm, are nearly half shallower than the conventional waveguide and have a TM mode field depth well satisfying the requirement by PhC fabrication. Such waveguide is promising for developing PhC devices, as well as other active and passive devices. In comparison with the conventional waveguide, the present shallow waveguide have slight larger waveguide loss and coupling loss. Nevertheless, with optimized fabrication parameters, the loss figure could be reduced to a lower level. Moreover, the device fabrication period could be shortened largely as the present shallow waveguide is employed. This is especially true for the case of developing an active device.

References

[1] M. Roussey, M. P. Bernal, N. Courjal, and F. I. Baida, "Experimental and theoretical characterization of a lithium niobate photonic crystal," *Appl. Phys. Lett.*, vol. 87, no. 24, p. 241 101, Dec. 2005.

[2] M. Roussey, M. P. Bernal, N. Courjal, D. Van Labeke, F. I. Baida, and R. Salut, "Electro-optic effect exaltation on lithium niobate photonic crystals due to slow photons," *Appl. Phys. Lett.*, vol. 89, no. 24, p. 241 110, Dec. 2006.

[3] G. Ulliac, N. Courjal, H. M. H. Chong, and R. M. De La Rue, "Batch process for the fabrication of $LiNbO_3$ photonic crystals using proton exchange followed by CHF_3 reactive ion etching," *Opt. Mater.*, vol. 31, no. 2, pp. 196–200, Oct.–Dec. 2008.

[4] H. Hu, R. Ricken, and W. Sohler, "Etching of lithium niobate: Micro- and nanometer structures for integrated optics," in *Proc. Topical Meeting—Photorefractive Materials, Effects, Devices—Control Light Matter*, Jun. 2009, pp. 1–2.

[5] M. Dinand and W. Sohler, "Theoretical modeling of optical amplification in Er-doped Ti:$LiNbO_3$ waveguides," *IEEE J. Quantum Electron.*, vol. 30, no. 5, pp. 1267–1276, May 1994.

[6] S. K. Korotky, W. J. Minford, L. L. Buhl, M. D. Divino, and R. C. Alferness, "Mode size and method for estimating the propagation constant of single-mode Ti:$LiNbO_3$ strip waveguides," *IEEE J. Quantum Electron.*, vol. QE-18, no. 10, pp. 1796–1801, Oct. 1982.
[7] G. W. Burr, S. Diziain, and M.-P. Bernal, "The impact of finite-depth cylindrical and conical holes in lithium niobate photonic crystals," *Opt. Exp.*, vol. 16, no. 9, pp. 6302–6316, Apr. 2008.
[8] M. Fukuma and J. Noda, "Optical properties of titanium-diffused $LiNbO_3$ strip waveguides and their coupling-to-a-fiber characteristics," *Appl. Opt.*, vol. 19, no. 4, pp. 591–597, Feb. 1980.
[9] S. Fouchet, A. Carenco, C. Daguet, R. Guglielmi, and L. Riviere, "Wavelength dispersion of Ti induced refractive index change in $LiNbO_3$ as a function of diffusion parameters," *J. Lightw. Technol.*, vol. LT-5, no. 5, pp. 700–708, May 1987.
[10] I. Baumann, R. Brinkmann, M. Dinand, W. Sohler, and S. Westenhöfer, "Ti:Er:$LiNbO_3$ waveguide laser of optimized efficiency," *IEEE J. Quantum Electron.*, vol. 32, no. 9, pp. 1695–1706, Sep. 1996.
[11] R. Regener and W. Sohler, "Loss in low-finesse Ti:$LiNbO_3$ optical waveguide resonators," *Appl. Phys. B, Lasers Opt.*, vol. 36, no. 3, pp. 143–147, Mar. 1985.
[12] U. Schlarb and K. Betzler, "Refractive indices of lithium niobate as a function of temperature, wavelength, and composition: A generalized fit," *Phys. Rev. B, Condens. Matter Mater. Phys.*, vol. 48, no. 21, pp. 15 613–15 620, Dec. 1993.
[13] Y. J. Ding and J. B. Khurgin, "A new scheme for efficient generation of coherent and incoherent submillimeter to THz waves in periodically-poled lithium niobate," *Opt. Commun.*, vol. 148, no. 1–3, pp. 105–109, Mar. 1998.
[14] G. Xu, X. Mu, Y. J. Ding, and I. B. Zotova, "Efficient generation of backward terahertz pulses from multiperiod periodically-poled lithium niobate," *Opt. Lett.*, vol. 34, no. 7, pp. 995–997, Apr. 2009.
[15] Y. J. Ding, "Efficient generation of far-infrared radiation from periodically-poled $LiNbO_3$ waveguide based on surface-emitting geometry," *J. Opt. Soc. Amer. B, Opt. Phys.*, vol. 28, no. 5, pp. 977–981, May 2011.
[16] P. R. Hua, D. L. Zhang, and E. Y. B. Pun, "Long period grating on strip Ti:$LiNbO_3$ waveguide embedded in planar Ti:$LiNbO_3$ waveguide," *IEEE Photon. Technol. Lett.*, vol. 22, no. 18, pp. 1361–1363, Sep. 2010.
[17] C. Becker, T. Oesselke, J. Pandavenes, R. Ricken, K. Rochhausen, G. Schreiberg, W. Sohler, H. Suche, R. Wessel, S. Balsamo, I. Montrosset, and D. Sciancalepore, "Advanced Ti:Er:$LiNbO_3$ waveguide lasers," *IEEE J. Sel. Topics Quantum Electron.*, vol. 6, no. 1, pp. 101–113, Jan./Feb. 2000.
[18] J. Amin, J. A. Aust, and N. A. Sanford, "Z-propagating waveguide lasers in rare-earth-doped Ti:$LiNbO_3$," *Appl. Phys. Lett.*, vol. 69, no. 25, pp. 3785–3787, Dec. 1996.
[19] C. H. Huang and L. McCaughan, "Photorefractive-damage-resistant Er-indiffused MgO:$LiNbO_3$ ZnO-waveguide amplifiers and lasers," *Electron. Lett.*, vol. 33, no. 19, pp. 1639–1640, Sep. 1997.
[20] B. K. Das, R. Ricken, V. Quiring, H. Suche, and W. Sohler, "Distributed feedback-distributed Bragg reflector coupled cavity laser with a Ti:(Fe:) Er:$LiNbO_3$ waveguide," *Opt. Lett.*, vol. 29, no. 2, pp. 165–167, Jan. 2004.
[21] G. Schreiber, D. Hofmann, W. Grundkotter, Y. L. Lee, H. Suche, V. Quiring, R. Ricken, and W. Sohler, "Nonlinear integrated optical frequency converters with periodically poled Ti:$LiNbO_3$ waveguides," in *Proc. SPIE*, 2001, vol. 4277, pp. 144–160.